Atmospheric record in the Hadean Eon from multiple sulfur isotope measurements in Nuvvuagittuq Greenstone Belt (Nunavik, Quebec)

Emilie A Thomassot, Jonathan O'Neil, Don Francis, Pierre A Cartigny, Boswell A Wing

Atmospheric record in the Hadean Eon from multiple sulfur isotope measurements in Nuvvuagittuq Greenstone Belt (Nunavik, Quebec)

Emilie Thomassot[a,b,c,1], Jonathan O'Neil[d], Don Francis[b], Pierre Cartigny[e], and Boswell A. Wing[b,c]

[a]Centre de Recherches Pétrographiques et Géochimiques, Université de Lorraine, 54501 Vandœuvre-Lès-Nancy, France; [b]Department of Earth and Planetary Sciences and [c]GEOTOP, McGill University, Montreal, QC H3A 0E8, Canada; [d]Department of Earth Sciences, University of Ottawa, Ottawa, ON K1N 6N5, Canada; and [e]Laboratoire de Géochimie des Isotopes Stables, Institut de Physique du Globe de Paris, UMR 7154 CNRS, Université Paris Denis-Diderot, Sorbonne Paris Cite, 75005 Paris, France

Edited by Mark H. Thiemens, University of California, San Diego, La Jolla, CA, and approved December 7, 2014 (received for review October 15, 2014)

Mass-independent fractionation of sulfur isotopes (S-MIF) results from photochemical reactions involving short-wavelength UV light. The presence of these anomalies in Archean sediments [(4–2.5 billion years ago, (Ga)] implies that the early atmosphere was free of the appropriate UV absorbers, of which ozone is the most important in the modern atmosphere. Consequently, S-MIF is considered some of the strongest evidence for the lack of free atmospheric oxygen before 2.4 Ga. Although temporal variations in the S-MIF record are thought to depend on changes in the abundances of gas and aerosol species, our limited understanding of photochemical mechanisms complicates interpretation of the S-MIF record in terms of atmospheric composition. Multiple sulfur isotope compositions ($\delta^{33}S$, $\delta^{34}S$, and $\delta^{36}S$) of the >3.8 billion-year-old Nuvvuagittuq Greenstone Belt (Ungava peninsula) have been investigated to track the early origins of S-MIF. Anomalous S-isotope compositions ($\Delta^{33}S$ up to +2.2‰) confirm a sedimentary origin of sulfide-bearing banded iron and silica-rich formations. Sharp isotopic transitions across sedimentary/igneous lithological boundaries indicate that primary surficial S-isotope compositions have been preserved despite a complicated metamorphic history. Furthermore, Nuvvuagittuq metasediments recorded coupled variations in $^{33}S/^{32}S$, $^{34}S/^{32}S$, and $^{36}S/^{32}S$ that are statistically indistinguishable from those identified several times later in the Archean. The recurrence of the same S-isotope pattern at both ends of the Archean Eon is unexpected, given the complex atmospheric, geological, and biological pathways involved in producing and preserving this fractionation. It implies that, within 0.8 billion years of Earth's formation, a common mechanism for S-MIF production was established in the atmosphere.

Nuvvuagittuq Greenstone Belt (Nunavik, Québec) | early Archean sulfur cycle | photochemistry | early Earth surface environment

Multiple sulfur isotopes have become the tool of choice for probing atmospheric evolution during the first 2.5 billion years of Earth history. In particular, mass-independent fractionation of sulfur isotopes (S-MIF) (1) is a characteristic feature of the geologic record before 2.32 gigayears ago (Ga) (2), after which S-MIF is almost completely lacking (3). Photochemistry in a low-O_2 atmosphere is often considered as the dominant cause of S-MIF (1), and models for production and preservation of S-MIF anomalies suggest that an increase in O_2 beyond $\sim 10^{-5}$ times present atmospheric level (PAL) (4) would quench the production of S-MIF signals in the geological record. While the abrupt nature of the Archean/Proterozoic transition reflects a high-sensitivity response to atmospheric O_2, the temporal variability of the S-MIF record before about 2.45 Ga indicates a complex interplay among atmospheric composition (5–8), magnitude (9) and oxidation state (10) of sulfur fluxes into the atmosphere, accessible photochemical pathways (11), microbial sulfur cycling in the surface environment (10), and atmospheric solar flux (12). Despite the broad range of geologic and biologic controls that apparently influence the S-isotopic record, first-order isotopic patterns are present that span wide intervals in time and are shared among a variety of rock-forming environments.

High-resolution measurements on Neoarchean samples (2.5–2.8 Ga) (13, 14) have provided evidence for temporal variation of the multiple S-isotopic signal reflecting changes in the relative proportions of atmospheric gases of volcanogenic and biogenic origin. The S-isotopic signal then appears as a robust metric of atmospheric composition that reflects both the photolytic reactions involving S-bearing phases and their transfer to the sediments. The present study focuses on the origins and extent of this atmospheric memory in the sedimentary record. To probe the sensitivity of early Archean photochemical processes to major surface perturbations, including emergence of dominant biogenic elemental cycling, intense volcanic activity, bombardment of Earth's surface by bolides, and evolution of the solar flux, we examined the multiple sulfur isotope record in some of the oldest metasediments found on Earth. The samples were collected in the >3.8-Ga Nuvvuagittuq Greenstone Belt (NGB) (15) located on the eastern coast of Hudson Bay (Ungava Penninsula, Northeastern Superior Province of Canada).

Geological Setting

The NGB exposes a sequence of metavolcanic rocks, ultramafic cumulates, and metasediments [primarily banded iron formations (BIF) and silica-rich formations (Si formation)] hosted in an isoclinal synform refolded into a south-plunging synform (*Supporting*

Significance

Sulfur isotopes in ancient Earth sediments have peculiar compositions resulting from photochemical reactions of sulfur-bearing gaseous species with UV photons in the anoxic early Earth's atmosphere. High-precision measurements of sediments from distinct localities have revealed that these isotopic anomalies are sensitive to the abundances of atmospheric gases. They thus appear as promising metrics of ancient atmospheric composition. In the present study, we focus on the origin and extent of this atmospheric memory. We analyzed the multiple S-isotope compositions of some of the oldest metasediments preserved on Earth (originating from the >3.8-Ga Nuvvuagittuq Greenstone Belt, Canada) and found that this unusual atmospheric fingerprint has been present since the end of the Hadean, the earliest eon of Earth history.

Author contributions: E.T. and B.A.W. designed research; E.T., J.O., D.F., P.C., and B.A.W. performed research; E.T. and P.C. contributed new reagents/analytic tools; E.T., J.O., D.F., P.C., and B.A.W. analyzed data; and E.T., J.O., D.F., P.C., and B.A.W. wrote the paper.

The authors declare no conflict of interest.

This article is a PNAS Direct Submission.

[1]To whom correspondence should be addressed. Email: emilie@crpg.cnrs-nancy.fr.

This article contains supporting information online at www.pnas.org/lookup/suppl/doi:10.1073/pnas.1419681112/-/DCSupplemental.

Information and Fig. S1). Samples from the predominant lithology in the belt [mafic amphibolites known as the Ujaraaluk unit (ref. 15 and *Supporting Information*)] as well as cogenetic ultramafic cumulate define a compact $^{142}Nd/^{144}Nd$ versus $^{147}Sm/^{144}Nd$ correlation. If interpreted as an isochron, the slope of this correlation corresponds to an age of 4.388 $^{+0.15}/_{-0.17}$ Ga (16), which would represent the emplacement age of the volcanic protolith to the Ujaraaluk unit (see *Supporting Information* for details on the Sm/Nd systematics and a discussion of this aspect). This Hadean age for the Ujaraaluk unit is strongly supported by the presence of gabbroic sills intruding the Ujaraaluk unit that yield a $^{143}Nd/^{144}Nd$ versus $^{147}Sm/^{144}Nd$ isochron age of 4.115 ± 0.1 Ga (16). Zircon from thin trondhjemitic intrusions (which sometimes occur as concordant horizons within the gabbroic sills) provide a minimum closure age of the U-Pb system [>3.75 Ga (17–20)]. These age relationships are consistent with the inferred intrusive relationships among the throndhjemite bands, the gabbro sills, and the amphibolite (15). Aluminous lithologies within the NGB contain mineral assemblages indicative of upper amphibolite facies metamorphism (*Supporting Information*), consistent with inferences from cation exchange thermometry [~640 °C (21)]. Precise U-Pb depth profiling of zircon grains indicates that this metamorphic grade was likely attained at ~2.7 Ga (21). The relative order of the BIF, Si formation, and volcanogenic horizons is symmetric across the synform, suggesting that the current lithological sequence reflects the original stratigraphy of the supracrustal package. The preservation of a coherent chemical stratigraphy within the Ujaraaluk unit supports this interpretation (15). Taken together, these observations suggest that deposition of the sediments was coeval with emplacement of the volcanic succession, which definitely occurred before 3.8 Ga, and may have been completed by 4.38 Ga.

Results: S-Isotope Signatures of NGB Rocks

The sulfur isotope compositions of our sample suite ($n = 39$) are divisible into two populations that correspond to broad lithological divisions (Table S1). Rocks interpreted to have igneous protoliths (ultramafic sills, gabbros with their intrusive felsic bands, or surrounding tonalites) have $\delta^{34}S$ values from −5.41‰ to 3.33‰ with a mean of 0.27 ± 2.37‰ (1σ) and a narrow range of $\Delta^{33}S$ values from −0.03‰ to 0.26‰, with a median value of 0.08‰ (*Supporting Information* and Table S2). These values are consistent with values reported for mantle-derived sulfur (ref. 22 and reference therein) with a minor contribution of S-MIF. In contrast, samples of inferred sedimentary origin ($n = 13$) have a tighter range of $\delta^{34}S$ values, from −1.64‰ to 3.18‰ associated with more dispersed and more significant nonzero S-MIF values ($+0.18‰ \leq \Delta^{33}S \leq +2.27‰$ and $-2.89‰ \leq \Delta^{36}S \leq -0.59‰$, Table S2). $\Delta^{33}S$ values of this second population are comparable with in situ data previously reported for Eoarchean metamorphic rocks of undisputed sedimentary origin (i.e., Isua BIF [$-0.25‰ \leq \Delta^{33}S \leq +3.41‰ \pm 0.22‰$ 1σ (23–25)] and Nuvvuagittuq Quartz-Biotite Schist [$+0.2‰ \leq \Delta^{33}S \leq +1‰$ (26)], both determined by Secondary Ion Mass Spectrometry).

The sulfur isotope anomalies in the BIF and Si formation from Nuvvuaggituq demonstrate that they contain sulfur that cycled through Earth's atmosphere before 3.8 Ga. This observation confirms the sedimentary origins of these lithologies (27). While metamorphic processes cannot create S-MIF, exchange or dilution with magmatic fluid would decrease its magnitude, and mixing with S-MIF bearing rocks would interfere with the initial signature. Evidence for a metamorphic event at ~2.7 Ga raises the possibility that original $\Delta^{33}S$ distribution in the NGB may have been modified through isotopic exchange between metasedimentary and metaigneous lithologies. Although there is no geologic evidence for the involvement of younger sediments in the 2.7-Ga metamorphic event, to assess the effect of possible reactive sulfur transport on $\Delta^{33}S$ values, we measured the perpendicular distance between every sampling location and the nearest major lithologic contact, and constructed a generalized profile of $\Delta^{33}S$ values versus distance from lithological contacts for the entire belt (Fig. 1). The profile reveals a step function in $\Delta^{33}S$ values, where the step coincides with the boundary between metasedimentary and metaigneous lithologies (Fig. 1). If reactive transport during metamorphism was an important process in resetting NGB $\Delta^{33}S$ systematics, there should be enhanced dispersion of $\Delta^{33}S$ values as the contact is approached, reflecting advective and/or diffusive modification of originally sharp isotopic gradients (28). Local evidence of isotopic disturbances of this type can be identified in mafic rocks in direct contact with the metasediments (greenstones or amphibolite, $n = 5$), which carry smaller, but nevertheless discernable, S-MIF anomalies ($-0.08‰ \leq \Delta^{33}S \leq 0.43‰$; $-1.74‰ \leq \Delta^{36}S \leq 0.54‰$), as well as clues of subsequent isotopic fractionation ($-0.33 < \delta^{34}S < 8‰$) (e.g., sample PC 189; Table S2). However, the overall morphology of the $\Delta^{33}S$ profile suggests that reactive transport was limited to restricted spatial scales (<2 m, Fig. 1). This enables us to interpret multiple S-isotope systematics in the NGB metasediments as robust indicators of the surface sulfur cycle at the time of deposition.

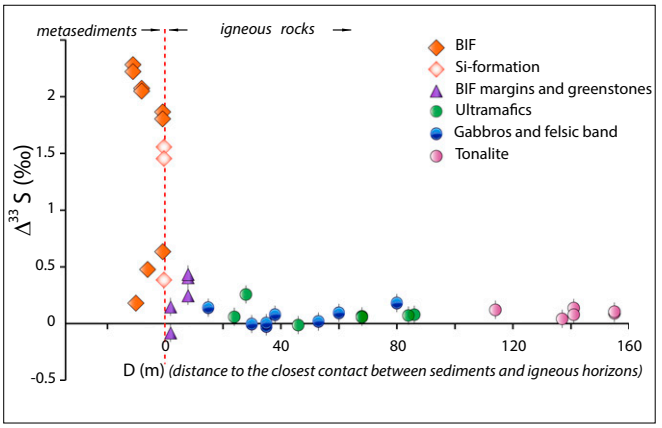

Fig. 1. Plot of sulfur mass-independent fractionation ($\Delta^{33}S$) versus distance to the nearest contact between proposed metasediments and metaigneous lithologies (D). BIF (filled orange diamonds) and Si formation (unfilled orange diamonds) all carry significant S-MIF anomalies, which confirm their sedimentary origin (when not plotted, the errors bars are smaller than the symbols). Metaigneous lithologies (gabbros, blue circles; ultramafic sills, green circles; surrounding tonalite, pink circles) do not show significant nonzero $\Delta^{33}S$. Small but discernable S-MIF anomalies identified in greenstones and on the BIF margins (lilac triangles) result from spatially limited reactive transport at the metasediment/metaigneous contact. The morphology of the $\Delta^{33}S$ profile (decreasing intensity with increasing D) is interpreted as evidence that the primary S-isotopic signal of the protoliths has been preserved.

Discussion

Structure of the Archean S-Isotopic Record. In rocks from the Archean Eon (2.50–3.85 Ga), anomalous ^{33}S enrichments (positive $\Delta^{33}S$) are commonly associated with ^{36}S depletions (negative $\Delta^{36}S$) and vice versa. Consequently, a compact negative correlation exists between $\Delta^{33}S$ and $\Delta^{36}S$ (*Supporting Information*). For much of the Archean Eon, this correlation is described by $\Delta^{36}S \approx -0.9 \times \Delta^{33}S$ (3). The breakdown of this relationship during the Mesoarchean Era (2.8–3.2 Ga) has been attributed to a global unique photochemical regime (11) driven by combination of a temporarily oxidizing atmosphere (29), high-altitude methane hazes leading to fluctuation in UV radiation transmitted through the atmosphere (30), and/or changes in H_2S/SO_2 of outgassed species (10). In addition, high-resolution data on Neoarchean (2.5–2.65 Ga) samples from both Australia and Africa (13, 14, 31, 32) show slight and stratigraphically controlled variations of $\Delta^{36}S/\Delta^{33}S$ from −0.9 to −1.5, reflecting

global perturbation of S-MIF source mechanisms. Changes in chemical composition of the atmosphere related to intense volcanism and biological CH_4 production, shortly before the irreversible atmospheric oxygenation, are thought to have caused these variations (33). Beyond these perturbations however, the $\Delta^{36}S/\Delta^{33}S$ value of −0.9 is common before 2.5 Ga, and may reflect a long-term temporal constancy of the atmospheric source mechanism that produced the anomalies. So far, in situ multiple S-isotope compositions of Eoarchean rocks (3.6–4 Ga) of sedimentary origin (i.e., Isua BIF) have shown preservation of nonzero $\Delta^{33}S$ anomalies (23–25), but in the absence of coupled ^{36}S quantification, it is unclear whether these S-MIF signals resemble those of the other Archean samples. Our results indicate that sulfides from Nuvvuagittuq BIF and Si-formation samples fall along a well-correlated array (Fig. 2*A*), a correlation which is not seen for metaigneous lithologies (*Supporting Information* and Fig. S2). The slope of this array (−0.85 ± 0.18) is statistically indistinguishable from that of the $\Delta^{36}S$ and $\Delta^{33}S$ array that characterizes the greater part of Archean atmospheric sulfur, outside of the $\Delta^{36}S/\Delta^{33}S$ ratios that are peculiar to the Mesoarchean [i.e., 2.8–3.2 Ga, Fig. 2*A* and Table S3]. Given the antiquity and geological history of the NGB, preservation of the canonical $\Delta^{36}S$–$\Delta^{33}S$ correlation is striking. The immediate inference is that within 800 million years of Earth's formation, and during the late heavy bombardment, an early mechanism for S-MIF production was established in the atmosphere. Comparison with both Paleoarchean (3.6–3.2 Ga) and Neoarchean (2.8–2.5 Ga) arrays (Fig. 2*A* and *Supporting Information*) suggests that this mechanism was extremely long lived, either sustained or revisited.

Furthermore, in a smaller subset of Archean sedimentary sulfides, recurrent patterns are observed for ^{34}S enrichments (or depletions) that consistently cooccur with anomalous ^{33}S enrichments (or depletions), leading to positive correlations between mass-independent sulfur isotope fractionation ($\Delta^{33}S$) and sulfur isotopic composition ($\delta^{34}S$) along slopes varying from 0.56 to 0.98 (9, 13, 34–36); see Table S3. As biological activity and geological mechanisms cause mass-dependent isotopic fractionation (and therefore modify $\delta^{34}S$ values) without affecting $\Delta^{33}S$, a linear $\Delta^{33}S$–$\delta^{34}S$ relationship is susceptible to modification and may become dispersed over time. Therefore, when preserved, $\Delta^{33}S$–$\delta^{34}S$ correlations are conventionally interpreted to be primary signatures, originating in the Archean atmosphere itself

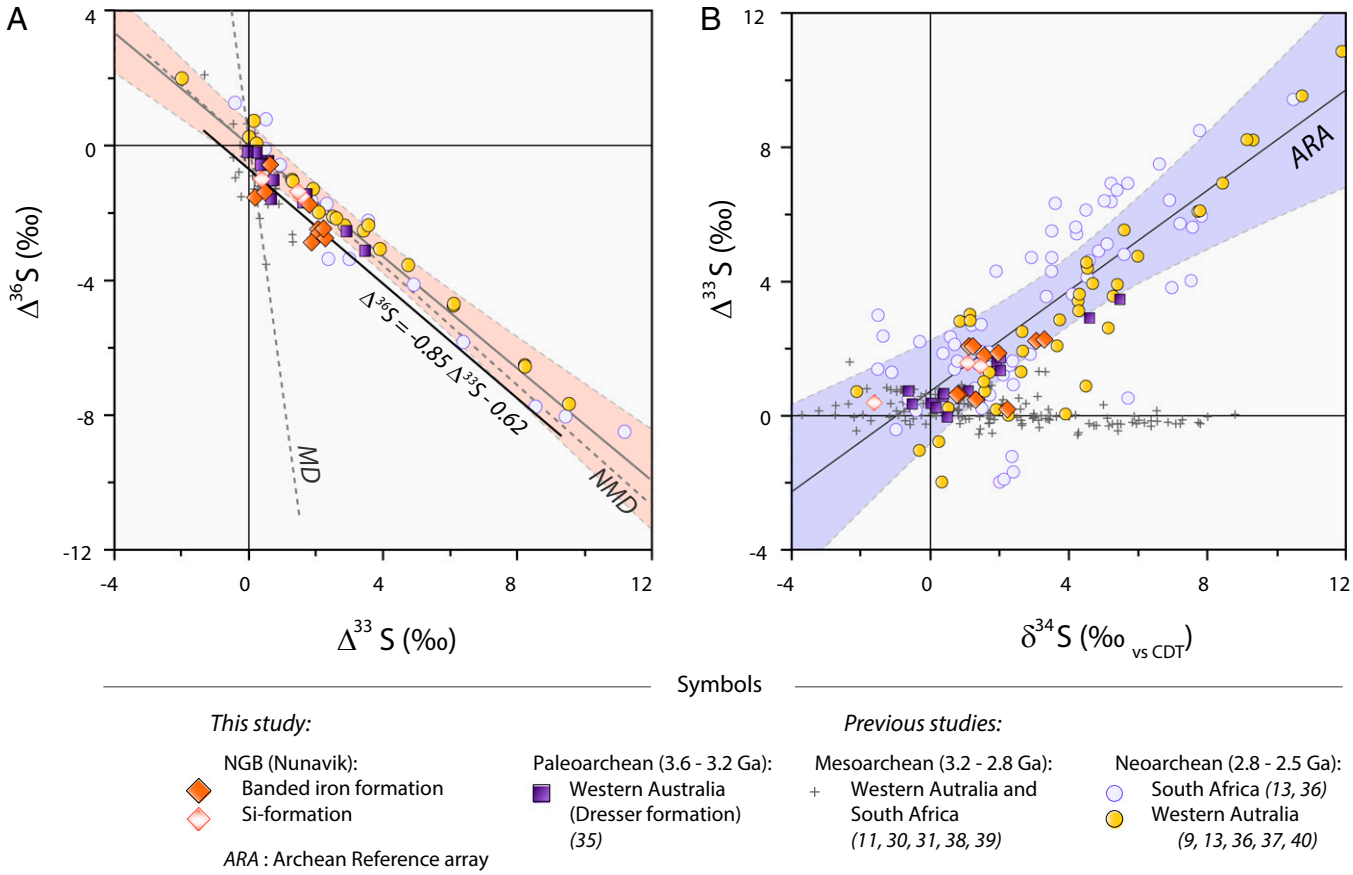

Fig. 2. (*A*) Triple sulfur isotope plot ($\Delta^{36}S$ versus $\Delta^{33}S$). NGB metasedimentary rocks [BIF samples, orange diamonds (n = 10); Si-formation samples, unfilled orange diamonds (n = 3)] are shown in comparison with Paleoarchean to Neoarchean samples [3.5 Ga: Western Australia, lilac squares (34); ∼2.5 Ga: South Africa (13, 35), unfilled blue circles; ∼2.5 Ga Western Australia (9, 13, 35, 36, 39), filled yellow circles; 2.7- to 3-Ga samples of diverse origins, gray crosses, (11, 29, 30, 37, 38)]. Neoarchean and Paleoarchean samples define a Non-Mass-Dependent array (dashed line, labeled as NMD) with a slope of ∼0.9 (3), which is distinct from the Mass-Dependent array [slope of ∼ −6.85 (3, 13), labeled as MD] expected for mass-dependent fractionation of ^{33}S and ^{36}S accompanying equilibrium fractionation. Data from NGB metasediments all have nonzero $\Delta^{33}S$ and $\Delta^{36}S$ and fall on a well-defined linear array ($\Delta^{36}S = -0.85\Delta^{33}S - 0.62$: black line) statistically indistinguishable from the NMD defined above (at the 99% confidence limit; light orange envelope). This similitude is interpreted as a record of an early-established, long-lived mechanism for S-MIF in the Archean atmosphere. (*B*) Plot of sulfur mass-independent fractionation ($\Delta^{33}S$) versus mass-dependent isotopic composition ($\delta^{34}S$). The Archean Reference array (dashed line labeled ARA) is defined by several well-preserved Archean formations of different ages and locations. NGB metasediments all fall within the 95% confidence band (light blue area) surrounding the ARA, whereas Mesoarchean samples, related to a specific photochemical regime (11, 29, 30, 37, 38), do not match this correlation.

(9). $\Delta^{33}S$ and $\delta^{34}S$ values reported here in metasediments exhibit a significant positive covariation [that is absent for metaigneous lithologies (*Supporting Information* and Fig. S3)], with all samples but one falling within the 95% confidence band of the correlation array preserved in several Neoarchean and Paleoarchean sedimentary intervals (Fig. 2*B*). Regression analysis of the NGB sulfur isotopes dataset yields a $\Delta^{33}S$–$\delta^{34}S$ slope of 0.71 (±0.13), which compares favorably with the pooled mean slope of all other younger examples of this correlation (0.73 ± 0.15; Table S3). We also conducted a more detailed time-integrated statistical comparison (Neoarchean, Mesoarchean, Paleoarchean, and Eoarchean) among published datasets and the present data by comparing slopes in $\Delta^{33}S$ vs. $\delta^{34}S$ space as determined from least-squares linear regression. The similarity of the slopes of the Neoarchean, Paleoarchean, and Eoarchean datasets was evaluated through nonequal variance *t* testing, because f tests indicated that the variance of the different datasets is not equal. Results indicate that the probability of equality of slopes is 61% between the 2.5–2.6-Ga and 3.5-Ga datasets, 64% between the 3.5-Ga sets and our study, and 78% between the 2.5–2.6-Ga datasets and our study.

There are two major conclusions from this exercise. First, the slope of the Mesoarchean dataset (2.7–3 Ga; data from refs. 11, 29, 30, 37, and 38) is not significantly different from 0 at the 99% confidence level. Second, there is a less than 1% probability of obtaining the observed trends in the Neoarchean dataset (2.5–2.6 Ga period; data from refs. 9, 13, 35, 36, and 39), Paleoarchean dataset (3.5 Ga; from ref. 34), and our data purely by chance from a dataset in which $\Delta^{33}S$ and $\delta^{34}S$ values do not covary. As has been inferred from $\Delta^{36}S$–$\Delta^{33}S$ relationships (11), these results indicate that the atmosphere in the Mesoarchean Era was clearly very different from the rest of the Archean. It is worth noting that a small subset of NGB metasedimentary samples display limited $\Delta^{33}S$ values associated with nonzero $\delta^{34}S$ and appear similar to Mesoarchean samples. This raises the possibility that atmospheric conditions during the formation of the NGB oscillated between those that were typical of most of the Archean and those that characterized the Mesoarchean. However, there is no compelling geological reason to select subsets of measurements from our dataset, which, unlike Mesoarchean samples, shows consistent $\Delta^{36}S$ and $\Delta^{33}S$ systematics (Fig. 2*A*). Mass-dependent isotopic fractionation during fluid circulation could be responsible for the increased $\delta^{34}S$ variability of these samples (Figs. S4 and S5). We consider the most reasonable interpretation to be that all the NGB sedimentary samples formed under the same environmental conditions.

Significance of S-Isotopic Trends in the Archean Rock Record. The slope of the $\Delta^{36}S$ vs. $\Delta^{33}S$ correlation is diagnostic of the overall reaction pathway leading to the formation of atmospheric sulfur species, irrespective of whether this relationship reflects fractionation during purely atmospheric processes (9) [including photodissociation (40) and/or photoexcitation (7)] or mixing of an atmospheric end-member(s) with unfractionated crustal sulfur [$\delta^{34}S \approx 0‰$, $\Delta^{33}S \approx 0‰$ (13)]. Sulfur isotope anomalies are produced by specific source mechanisms among which the photodissociation of the SO_2 molecule by high-energy photons (in the 185- to 220-nm absorption region) has been most thoroughly explored. Experimental and theoretical studies show that photolytic S-MIF production and its transfer into sediments imply a restricted compositional range in several atmospheric species. Oxygen levels above 10^{-2} times PAL induce the formation of an ozone shield for UV radiation, minimizing SO_2 photolysis and thus preventing the production of the anomaly, thereby setting an upper limit on oxygen levels (41). Preservation of the anomaly within the atmospheric column requires even lower oxygen levels [$<10^{-5}$ PAL (4)] to prevent the rapid back reaction of the anomalous atomic sulfur to oxidized atmospheric species and to allow the transfer of S-MIF to sediments. Isotopic fractionation during H_2S photochemistry is only weakly anomalous (1, 10). The SO_2/H_2S ratio of volcanic gases entering the atmosphere, therefore, must have been high enough [with SO_2 flux at least equal to the high modern level, estimated to be close to 1×10^{12} mol y^{-1} (5, 9)] to prevent the dilution of the isotopic anomaly by weakly MIF-fractionated H_2S.

In addition to the essential conditions described above, isotopic studies of Neoarchean (2.5–2.6 Ga) sediments from several localities, coupled with atmospheric modeling, mostly indicate that atmospheric O_2 and CH_4 levels are the primary controls on sulfur flow through the elemental sulfur reaction network (5, 9, 14): A CH_4/CO_2 ratio of 0.01 best accounts for the highest SO_2 photolysis rates in an haze-free atmosphere (30), whereas enhanced methane flux would decrease this rate (14). Consequently CH_4 and CO_2 abundances substantially influence the slope of $\Delta^{36}/\Delta^{33}S$ (9, 14, 33). It is worth noting that biogeochemical models commonly link oxygenation of the atmosphere through time to integrated hydrogen escape, enhanced by CH_4-producing biological activity [i.e., methanogenesis (42)]. Accordingly, if the fluxes of O_2 and CH_4 to the Archean atmosphere were biologically controlled, this may argue for a close relationship between the production of the S-MIF arrays and biological activity. Given the diversity of the evidence for a thriving microbial biosphere in the Neoarchean [coupled isotope fractionation records, organic biomarkers, metal chemistry in black shales (13, 39)], the assumption of a strong biological influence on the atmospheric production of S-isotopic record seems valid for this period. However, extending the uniformitarian interpretation of a biological influence on the S-MIF arrays seen in our samples is risky in the absence of any other independent biomarkers at Nuvvuagittuq (43), and likely incorrect given the metabolic innovation that seems to have occurred throughout the Archean. The preservation of the $\Delta^{33}S$–$\delta^{34}S$ Archean reference array in the sedimentary record requires a relatively weak biological sulfur cycle to avoid the isotopic homogenization that occurs during microbial sulfur reduction (44). The trends reported here ($\Delta^{33}S/\delta^{34}S \approx 0.7$, Fig. 2) thus suggest that the atmospheric signal has been little modified by biological activity after deposition and rather indicates that microbial S cycling, if it was present at all, was not a significant component of the Nuvvuagittuq sedimentary environment (10, 44). If a shared biogenic control on the S-MIF record at both the beginning and the end of the Archean Eon is unlikely, recurrent gas inputs in the atmosphere by magmatic activity may be able to produce comparable photochemical pathways at any time in the Archean (45–47). Such a strong geological control on S-MIF record would then be decoupled from singular events like the emergence of biogenically dominated element cycling or intense bombardments by meteorites. Trends in S-MIF may thus represent atmospheric signatures resulting from volcanologically induced atmospheric mechanisms, among which SO_2 photolysis has been studied in greatest detail so far.

Implication for Early S-MIF Source Mechanisms. S-MIF production by SO_2 photolysis in the 185- to 220-nm region is supported by experimental studies that reveal its sensitivity to gas composition (41), UV wavelength (48), and gas pressure (49), implying that $\Delta^{33}S$ and $\delta^{34}S$ values should be responsive to the local atmospheric state. However, some important issues remain unresolved because photodissociation alone does not provide a complete quantitative explanation of the S-MIF signatures in the rock record (50). In Archean sediments, S-MIF anomalies (up to ~12‰ at the end of the Archean Eon) are associated with minor mass-dependent isotopic fractionation (leading to the $\Delta^{33}S/\delta^{34}S$ trend ≈ 0.7) whereas photolysis experiments under a wide range of pSO_2, light sources, and bath gas compositions exclusively produce significant $\Delta^{33}S$ (of about 20‰) only when isotopic fractionation is large ($\delta^{34}S$ up to 180‰) leading to $\Delta^{33}S/\delta^{34}S < 0.1$, far lower than the recurrent Archean array also reported here. In addition to the experimental

data, the most sophisticated numerical models for accurately calculating the magnitude and sign of mass-independent fractionations in the Archean atmosphere complicate the problem. They predict $\Delta^{33}S$ at odds with the geological records [i.e., positive $\Delta^{33}S$ associated with sulfate but with elemental sulfur (51)]. As sulfur dioxide photodissociation rates are related to the actinic flux, this type of numerical approach also indicates that under the flux of the 4.2-Ga Sun, this rate has been 38–48% lower (ref. 12) than those computed assuming a modern Sun (13, 14, 32, 40), questioning the relevance of considering SO_2 photodissociation as a lasting S-MIF source mechanism through time.

Apart from simple photodissociation (i.e., in the ~200-nm broadband and without shielding), alternative atmospheric mechanisms can create significant S-MIF (50). Recent numerical and experimental studies report specific isotopic trends in both $\Delta^{33}S/\Delta^{36}S$ and $\delta^{34}S/\Delta^{33}S$ for (*i*) photodissociation with self-shielding in a SO_2–N_2 bath gas [$\Delta^{36}/\Delta^{33}S = -4.6 \pm 1.3$, $\Delta^{33}S/\delta^{34}S = +0.086 \pm 0.035$ (45)], (*ii*) simple photoexcitation [$\Delta^{36}/\Delta^{33}S = -2$ to -3, $\Delta^{33}S/\delta^{34}S \approx +0.5$ (7)], and (*iii*) photoexcitation of self-shielded SO_2 molecules in the 240- to 350-nm range [positive $\Delta^{36}/\Delta^{33}S$, from $+0.64 \pm 0.3$ (8) to +2.25 (52) and $\Delta^{33}S/\delta^{34}S$ from ~+1 (8) to +3 (45)]. In addition to the nature of the photoreaction processes, the presence of reduced species (such as carbon monoxide) can modify the $\Delta^{33}S/\delta^{34}S$ relationship, as such species have been shown to be competing absorbers that considerably affect photoreaction rates (8). However, in the absence of sufficient quantitative constraints on S-MIF production under reduced atmospheric conditions (e.g., quantum mechanical treatments), there is no evidence that any of these mechanisms could alone account for the isotopic composition of Archean sediments. Considering similar issues in the modern environment, it is worth noting that numerical modeling of SO_2 photoexcitation in the region of 250–320 nm matches the isotopic variations preserved in modern sulfate-rich horizons in polar ice cores and snowpacks (7). These materials record stratospheric chemical processing of SO_2-rich plumes from a wide range of Plinian volcanic eruptions and are characterized by a robust positive $\Delta^{33}S$–$\delta^{34}S$ correlation, coupled with negative $\Delta^{33}S/\Delta^{36}S$ trends [$\Delta^{33}S/\delta^{34}S \approx 0.1$; $\Delta^{36}S/\Delta^{33}S \approx -2$ to -3 (ref. 53 and references therein)]. For photoexcited SO_2, isotopologue-specific excitation rates result from the coupled effect of actinic flux with the slight shift on the absorption cross section between isotopes (48) and lead to wavelength-dependent isotopic fractionation. For photoexcited SO_2, the actinic flux of low-energy photons that controls the magnitude of the isotopic effect (>290 nm) becomes dominant below 30 km (because 220- to 290-nm wavelengths are absorbed at higher altitude by O_3). Accordingly, a correlation between isotopic fractionation and altitude is predicted in the numerical models and fits with the observed $\Delta^{33}S/\Delta^{36}S$ trend (7). Although the combined slopes of the Archean $\Delta^{33}S$–$\Delta^{36}S$–$\delta^{34}S$ correlations formed under different atmospheric conditions from recent plumes, they exhibit a comparable scale of variability (10). So far, SO_2 photoexcitation has been little explored, especially in reduced atmospheres for which the chemical reaction network is poorly constrained. However, these atmospheric conditions may allow S-MIF transfer to the sulfate aerosols: $^*SO_2 + SO_2 \rightarrow SO_3 + SO$ and $SO_3 + H_2O \rightarrow H_2SO_4$.

This type of mechanism would imply a strong geological control on S-MIF production related to dramatic volcanic eruptions and may provide an explanation for the recurrence of the S-MIF signal over a long period despite major changes in biogenic gas release into the atmosphere. More generally, regardless of the exact S-MIF source mechanisms involved, the recurrent S-MIF isotopic trend over the Archean suggests that either different combinations of atmospheric, geological, and biological pathways could produce the same S-isotope pattern or similar states of the Earth surface system were revisited several times in Archean history. Major episodes of volcanic eruption and outgassing could plausibly provide a recurrent SO_2-rich Archean atmosphere, potentially producing similar S-isotopic fractionation trends over time.

Methods

Sulfur isotope analyses required multiple steps of extraction and purification before mass spectrometry. Powdered whole rock samples were reacted at ~85 °C with a Cr-reducing solution (54) that liberated H_2S from sulfide grains. This H_2S was subsequently converted to Ag_2S by trapping the H_2S in a 10% (wt/wt) zinc acetate solution and reacting the resulting ZnS with a 0.2 M $AgNO_3$ solution. The Ag_2S was then reacted in a nickel reaction vessel overnight at ~250 °C in the presence of excess F_2 to produce SF_6. The resulting SF_6 was purified first cryogenically and then with a gas chromatograph. Purified SF_6 was introduced into a ThermoFinnigan MAT 253 dual-inlet gas-source mass spectrometer where sulfur isotope abundances were measured by monitoring the $^{32}SF_5^+$, $^{33}SF_5^+$, $^{34}SF_5^+$, and $^{36}SF_5^+$ ion beams at mass to charge ratios of m/z = 127, 128, 129, and 131, respectively. All sulfur isotope data are reported relative to Vienna Cañon Diablo Troilite (V-CDT). The external reproducibility (1σ) for the full measurement procedure (extraction, fluorination, and mass spectrometry) is estimated to be better than 0.1‰ for $\delta^{34}S$ values and 0.01‰ and 0.1‰ for $\Delta^{33}S$ values and $\Delta^{36}S$ values, respectively, as based on both the measurement of the Ag_2S international standard from the International Atomic Energy Agency (IAEA)-S1 and an in-house rock sample. Our results on IAEA standards agree, within error, with those previously reported (table 2 in ref. 37).

ACKNOWLEDGMENTS. We thank the municipality of Inukjuak and the Pituvik Landholding Corporation for permission to work on their territory, as well as Mike Carroll and Minnie and Noah Echalook for their hospitality and support. Yumi Kitayama is thanked for her help in the field and for numerous scientific discussions. We thank Laurie Reisberg, Eric Hebrard, Sebastian Danielache, and Vincent Van Hinsberg for their constructive reviews of the manuscript, Michel Fialin for his assistance during electron-probe measurements, as well as Mary Ford and Gaston Giuiliani for their support. This research was supported by National Science and Engineering Research Council of Canada Discovery grants (to D.F. and B.A.W.), a Canadian Space Agency–Canadian Analogue Research Network grant (to B.A.W.), the region Lorraine (Bourses régionales soutient aux jeunes chercheurses to E.T.), and the Centre National de la Recherche Scientifique (via their program "Environnements planétaires et origines de la vie" to E.T.).

1. Farquhar J, Bao H, Thiemens M (2000) Atmospheric influence of Earth's earliest sulfur cycle. *Science* 289(5480):756–759.
2. Bekker A, et al. (2004) Dating the rise of atmospheric oxygen. *Nature* 427(6970): 117–120.
3. Johnston DT (2011) Multiple sulfur isotopes and the evolution of Earth's surface sulfur cycle. *Earth Sci Rev* 106(1-2):161–183.
4. Pavlov AA, Kasting JF (2002) Mass-independent fractionation of sulfur isotopes in Archean sediments: Strong evidence for an anoxic Archean atmosphere. *Astrobiology* 2(1):27–41.
5. Zahnle K, Claire M, Catling D (2006) The loss of mass-independent fractionation in sulfur due to a Palaeoproterozoic collapse of atmospheric methane. *Geobiology* 4(4):271–283.
6. Ueno Y, et al. (2009) Geological sulfur isotopes indicate elevated OCS in the Archean atmosphere, solving faint young sun paradox. *Proc Natl Acad Sci USA* 106(35): 14784–14789.
7. Hattori S, et al. (2013) SO_2 photoexcitation mechanism links mass-independent sulfur isotopic fractionation in cryospheric sulfate to climate impacting volcanism. *Proc Natl Acad Sci USA* 110(44):17656–17661.
8. Whitehill A, Ono S (2012) Excitation band dependence of sulfur isotope mass-independent fractionation during photochemistry of sulfur dioxide using broadband light sources. *Geochim Cosmochim Acta* 94:238–253.
9. Ono S, Eigenbrode JL, Pavlov AA, Kharecha P, Rumble D, Kasting JF, Freeman KH (2003) New insights into Archean sulfur cycle from mass-independent sulfur isotope records from the Hamersley Basin, Australia. *Earth Planet Sci Lett* 213(1-2): 15–30.
10. Halevy I, Johnston DT, Schrag DP (2010) Explaining the structure of the Archean mass-independent sulfur isotope record. *Science* 329(5988):204–207.
11. Farquhar J, et al. (2007) Isotopic evidence for Mesoarchaean anoxia and changing atmospheric sulphur chemistry. *Nature* 449(7163):706–709.
12. Claire M, et al. (2012) The evolution of solar flux from 0.1 nm to 160 μm: Quantitative estimates for planetary studies. *Astrophys J* 757(1):95–107.
13. Kaufman AJ, et al. (2007) Late Archean biospheric oxygenation and atmospheric evolution. *Science* 317(5846):1900–1903.
14. Zerkle A, et al. (2012) A bistable organic-rich atmosphere on the Neoarchaean Earth. *Nat Geosci* 5(5):359–363.

15. O'Neil J, Francis D, Carlson R (2011) Implications of the Nuvvuagittuq Greenstone Belt for the formation of Earth's early crust. *J Petrol* 52(5):985–1009.
16. O'Neil J, Carlson R, Paquette J, Francis D (2012) Formation age and metamorphic history of the Nuvvuagittuq Greenstone Belt. *Precambrian Res* 220–221:23–44.
17. Cates N, Mojzsis S (2007) Pre-3750 Ma supracrustal rocks from the Nuvvuagittuq supracrustal belt, northern Quebec. *Earth Planet Sci Lett* 255(1-2):9–21.
18. David J, Godin L, Stevenson R, O'Neil J, Francis D (2009) U-Pb ages (3.8–2.7 Ga) and Nd isotope data from the newly identified Eoarchean Nuvvuagittuq supracrustal belt, Superior Craton, Canada. *Geol Soc Am Bull* 121(1-2):150–163.
19. Darling JR, et al. (2013) Hadean to Neoarchaean evolution of the Nuvvuagittuq greenstone belt: New insights from U-Pb zircon geochronology. *Am J Sci* 313:844–876.
20. O'Neil J, Boyet M, Carlson RW, Paquette J-L (2013) Half a billion years of reworking of Hadean mafic crust to produce the Nuvvuagittuq Eoarchean felsic crust. *Earth Planet Sci Lett* 379:13–25.
21. Cates N, Mojzsis S (2009) Metamorphic zircon, trace elements and Neoarchean metamorphism in the ca. 3.75 Ga Nuvvuagittuq supracrustal belt, Quebec (Canada). *Chem Geol* 261(1-2):98–113.
22. Labidi J, Cartigny P, Hamelin C, Moreira M, Dosso D (2014) Sulfur isotope budget (^{32}S, ^{33}S, ^{34}S and ^{36}S) in Pacific–Antarctic ridge basalts: A record of mantle source heterogeneity and hydrothermal sulfide assimilation. *Geochim Cosmochim Acta* 133:47–67.
23. Papineau D, Mojzsis SJ (2006) Mass-independent fractionation of sulfur isotopes in sulfides from the pre-3770 Ma Isua Supracrustal Belt, West Greenland. *Geobiology* 4(4):227–238.
24. Whitehouse M, Kamber B, Fedo C, Lepland A (2005) Integrated Pb- and S-isotope investigation of sulphide minerals from the early Archaean of southwest Greenland. *Chem Geol* 222(1-2):112–131.
25. Mojzsis S, Coath J, Greenwood K, McKeegan K, Harrison T (2003) Mass-independent isotope effects in Archean (2.5 to 3.8 Ga) sedimentary sulfides determined by ion microprobe analysis. *Geochim Cosmochim Acta* 67(9):1635–1658.
26. Kitayama Y, Thomassot E, O'Neil J, Wing B (2012) Sulfur-and oxygen-isotope constraints on the sedimentary history of apparent conglomerates from the Nuvvuagittuq Greenstone Belt (Nunavik, Québec). *Earth Planet Sci Lett* 355-356:271–282.
27. Dauphas N, Cates N, Mojzsis S, Busigny V (2007) Identification of chemical sedimentary protoliths using iron isotopes in the > 3750 Ma Nuvvuagittuq supracrustal belt, Canada. *Earth Planet Sci Lett* 254(3-4):358–376.
28. Penniston-Dorland S, et al. (2008) Multiple sulfur isotopes reveal a magmatic origin for the Platreef platinum group element deposit, Bushveld Complex, South Africa. *Geology* 36(12):979–982.
29. Ohmoto H, Watanabe Y, Ikemi H, Poulson SR, Taylor BE (2006) Sulphur isotope evidence for an oxic Archaean atmosphere. *Nature* 442(7105):908–911.
30. Domagal-Goldman SD, Kasting JF, Johnston DT, Farquhar J (2008) Organic haze, glaciations and multiple sulfur isotopes in the Mid-Archean Era. *Earth Planet Sci Lett* 269(1-2):29–40.
31. Thomazo C, Nisbet E, Grassineau N, Peters M, Strauss H (2013) Multiple sulfur and carbon isotope composition of sediments from the Belingwe Greenstone Belt (Zimbabwe): A biogenic methane regulation on mass independent fractionation of sulfur during the Neoarchean? *Geochim Cosmochim Acta* 121:120–138.
32. Kurzweil F, et al. (2013) Atmospheric sulfur rearrangement 2.7 billion years ago: Evidence for oxygenic photosynthesis. *Earth Planet Sci Lett* 366:17–26.
33. Ueno Y, Endo Y, Mishima K, Danielache SO (2014) Decoding the evolution of early atmosphere: Experimental reconstruction of the $\Delta^{36}S/\Delta^{33}S$ chemostratigraphy. *Proceedings of the Japan Goscience Union Meeting 2014* (Jpn Geosci Union, Tokyo, Japan).
34. Ueno Y, Ono SH, Rumble D, Maruyama S (2008) Quadruple sulfur isotope analysis of ca. 3.5 Ga Dresser Formation: New evidence for microbial sulfate reduction in the early Archean. *Geochim Cosmochim Acta* 72(23):5675–5691.
35. Ono SH, Beukes NJ, Rumble D (2009) Origin of two distinct multiple-sulfur isotope compositions of pyrite in the 2.5 Ga Klein Naute Formation, Griqualand West Basin, South Africa. *Precambrian Res* 169(1-4):48–57.
36. Partridge MA, Golding SD, Baublys KA, Young E (2008) Pyrite paragenesis and multiple sulfur isotope distribution in late Archean and early Paleoproterozoic Hamersley Basin sediments. *Earth Planet Sci Lett* 272(1-2):41–49.
37. Thomazo C, Ader M, Farquhar J, Philippot P (2009) Methanotrophs regulated atmospheric sulfur isotope anomalies during the Mesoarchean (Tumbiana Formation, Western Australia). *Earth Planet Sci Lett* 279(1-2):65–75.
38. Ono SH, Wing BA, Johnston D, Farquhar J, Rumble D (2006) Mass-dependent fractionation of quadruple stable sulfur isotope system as a new tracer of sulfur biogeochemical cycles. *Geochim Cosmochim Acta* 70(9):2238–2252.
39. Ono SH, Kaufman AJ, Farquhar J, Sumner DY, Beukes NJ (2009) Lithofacies control on multiple-sulfur isotope records and Neoarchean sulfur cycles. *Precambrian Res* 169(1-4):58–67.
40. Lyons JR (2007) Mass-independent fractionation of sulfur isotopes by isotope-selective photodissociation of SO_2. *Geophys Res Lett* 34(22):L22811.
41. Farquhar J, Savarino J, Airieau S, Thiemens MH (2001) Observation of wavelength-sensitive mass-independent sulfur isotope effects during SO_2 photolysis: Implications for the early atmosphere. *J Geophys Res* 106(E12):32829–32839.
42. Claire MW, Catling DC, Zahnle KJ (2006) Biogeochemical modelling of the rise in atmospheric oxygen. *Geobiology* 4(4):239–269.
43. Papineau D, et al. (2011) Young poorly crystalline graphite in the > 3.8-Gyr-old Nuvvuagittuq banded iron formation. *Nat Geosci* 4(6):376–379.
44. Halevy I (2013) Production, preservation, and biological processing of mass-independent sulfur isotope fractionation in the Archean surface environment. *Proc Natl Acad Sci USA* 110(44):17644–17649.
45. Ono S, Whitehill AR, Lyons JR (2013) Contribution of isotopologue self-shielding to sulfur mass-independent fractionation during sulfur dioxide photolysis. *J Geophys Res* 118(5):2444–2454.
46. Philippot P, Van Zuilen M, Rollion-Bard C (2012) Variations in atmospheric sulphur chemistry on early Earth linked to volcanic activity. *Nat Geosci* 5(5):668–674.
47. Shaheen R, et al. (2014) Large sulfur-isotope anomaly in nonvolcanic sulfate aerosol and its implications for the Archean atmosphere. *Proc Natl Acad Sci USA* 111(33): 11979–11983.
48. Danielache SO, Eskebjerg C, Johnson MS, Ueno Y, Yoshida N (2008) High-precision spectroscopy of S^{-32}, S^{-33}, and S^{-34} sulfur dioxide: Ultraviolet absorption cross sections and isotope effects. *J Geophys Res, D, Atmospheres* 113(D17):D17314.
49. Masterson AL, Farquhar J, Wing BA (2011) Sulfur mass-independent fractionation patterns in the broadband UV photolysis of sulfur dioxide: Pressure and third body effects. *Earth Planet Sci Lett* 306(3-4):253–260.
50. Lyons JR (2009) Atmospherically-derived mass-independent sulfur isotope signature, and incorporation into sediments. *Chem Geol* 267(3-4):164–174.
51. Claire MA, et al. (2014) Modeling the signature of sulfur mass-independent fractionation produced in the Archean atmosphere. *Geochim Cosmochim Acta* 141: 365–380.
52. Whitehill AR, et al. (2013) Vibronic origin of sulfur mass-independent isotope effect in photoexcitation of SO_2 and the implications to the early Earth's atmosphere. *Proc Natl Acad Sci USA* 110(44):17697–17702.
53. Baroni M, Savarino J, Cole-Dai J, Rai V, Thiemens M (2008) Anomalous sulfur isotope compositions of volcanic sulfate over the last millennium in Antarctic ice cores. *J Geophys Res* 113(D20):D20112.
54. Canfield DE, Raiswell R, Westrich JT, Reaves CM, Berner RA (1986) The use of chromium reduction in the analysis of reduced inorganic sulfurin sediments and shales. *Chem Geol* 54(1-2):149–155.